WHOI-93-23
c.1

Woods Hole Oceanographic Institution

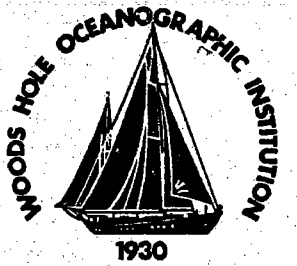

Design Study for a Moored Surface-Scanning Sonar

by

Lee E. Freitag, Albert J. Plueddemann, and Steve Merriam

June 1993

Technical Report

Funding was provided by a grant from the Webster Foundation to the Woods Hole Oceanographic Institution

WHOI-93-23

Design Study for a Moored Surface-Scanning Sonar

by

Lee E. Freitag, Albert J. Plueddemann, and Steve Merriam

Woods Hole Oceanographic Institution
Woods Hole, Massachusetts 02543

June 1993

Technical Report

Funding was provided by a grant from the Webster Foundation to the Woods Hole Oceanographic Institution

Approved for Distribution:

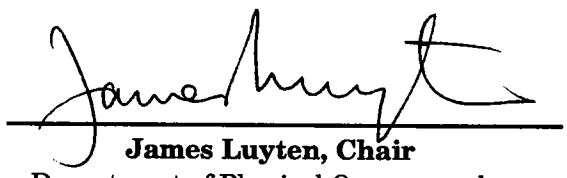

James Luyten, Chair
Department of Physical Oceanography

Abstract

This report contains the results of a design study for a surface scanning sonar instrument capable of long-term deployment on ocean moorings. The instrument is intended to sample the bubble field just below the ocean's surface and compute the backscattered intensity and Doppler velocity in small unit volumes. The principal motivation for the development of such an instrument is to enhance the study of upper ocean processes by utilizing the ability of the sonar to detect surface waves and Langmuir circulation. Important design parameters for the instrument are investigated and a detailed design proposed. Key technical issues such as the trade-offs among spatial resolution, temporal resolution, velocity precision, total range, and power are discussed. The azimuthal motion of the instrument on a mooring is considered as a potential problem, and possible solutions are discussed. Matlab functions used for the investigations are included in an appendix.

Table of Contents

Introduction 1
Background 1
Approach 3

System Parameter Analysis 6
Transducer & Signals 6
Maximum Attainable Source Level 8
Sonar Equations: Estimated SNR 10
Velocity Estimation 13
Velocity Estimates Using Coded Waveforms 15
Summary of System Specifications 15
Sampling Strategies 17

Impact of Mooring Motion on the Instrument 19
Impact on Directional Wave Spectra 19
Impact on Sidescan Intensity Measurements 19
Impact on Doppler Measurements for Langmuir Circulation 20
Motion Compensation 21

Electrical And Mechanical Systems 22
System Operation 22
Doppler Sonar System Description 22
Mechanical Layout and Transducers 22
Electronics Systems 23
Data Storage 25
Sensors 25

Acknowledgments 26

References and Bibliography 27

Appendix 29

1.0 Introduction

1.1 Background

Recent developments in the use of surface-scanning sonars to image the underside of the sea surface have resulted in new techniques for the observation of ocean surface waves, the detection of wave- induced bubble clouds, and the measurement of near-surface currents associated with Langmuir circulation (Pollard, 1977; Leibovich, 1983). Thorpe and his collaborators (e.g. Thorpe and Hall, 1983; Thorpe, et al., 1985) showed that a sonar with a frequency near 250 kHz was able to detect bubble clouds generated by surface waves. These clouds are made up of microbubbles with radii from 20-400 microns generated by whitecapping and wave breaking. The microbubbles persist below the surface much longer than the whitecaps observed at the surface, which have a lifetime of only a few seconds. The bubbles remain strongly surface trapped with a profile roughly equivalent to exponential decay with a depth scale of order 1 to 3 meters depending on the wind speed (Thorpe, 1986; Crawford and Farmer, 1987). In winds over 3-4 mps the bubbles form a nearly continuous near-surface layer and dominate acoustic backscatter over a range of frequencies between about 10 kHz and several hundred kHz.

Surface-scanning sonars have beam patterns which are narrow azimuthally, but broad in the vertical. At any given range the total insonified volume describes a narrow, but deep, element of spherical surface approximating an arc. However, the vertical extent of the measurement volume is confined to a thin layer near the surface by the nature of the bubble layer (Figure 1). There is no discrimination as to the depth of the targets in the processing; the above interpretation of the measurement volume is based on the knowledge that the bubble clouds are confined to the surface layer and the fact that the backscatter due to bubbles far exceeds that from the sea surface (as well as that from the deeper, bubble-free water) at small incidence angles. Based on the depth scale of the bubble layer, the vertical extent of the measurement volume is taken to be from 2 to 3 meters, from the surface downward. The extent of the measurement volume in range is determined by the duration of transmitted pulse and the amount of range-averaging, while the azimuthal dimension is set by the azimuthal beam width. The beam geometry minimizes sensitivity to pitch and roll of the platform, while maintaining a small measurement volume just below the ocean surface, and following the vertical excursions of the fluid (a water-bubble mixture) there. The resulting measurements are "semi-Lagrangian," following fluid parcels in the vertical but not in the horizontal directions.

Although Thorpe's initial studies were undertaken to examine the distribution of bubble clouds and the process of wave breaking, it was recognized that the acoustically imaged bubbles acted as tracers of fluid motion in the upper few meters of the sea. Thus, by adding Doppler capability to a surface-scanning sonar similar to that used by Thorpe, it was possible to detect the orbital motion of surface waves and the near-surface currents associated with Langmuir circulation. The acoustical visualization of Langmuir circulation arises from clouds of small bubbles presumed to be injected into the surface layer at random locations by breaking waves, and then drawn into Langmuir cell convergence zones by near-surface currents. A surface-scanning sonar directed perpendicular to the wind direc-

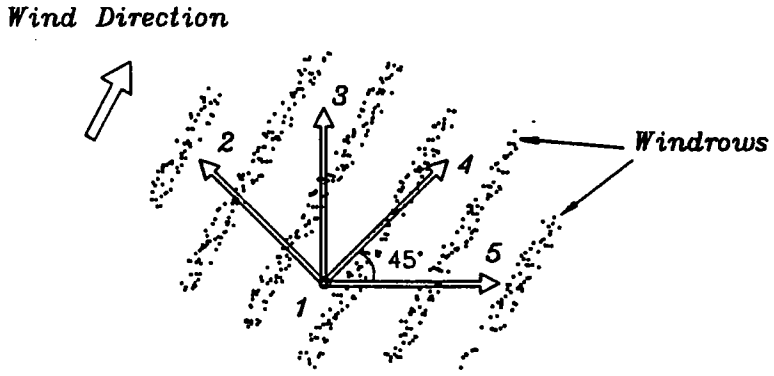

Top View

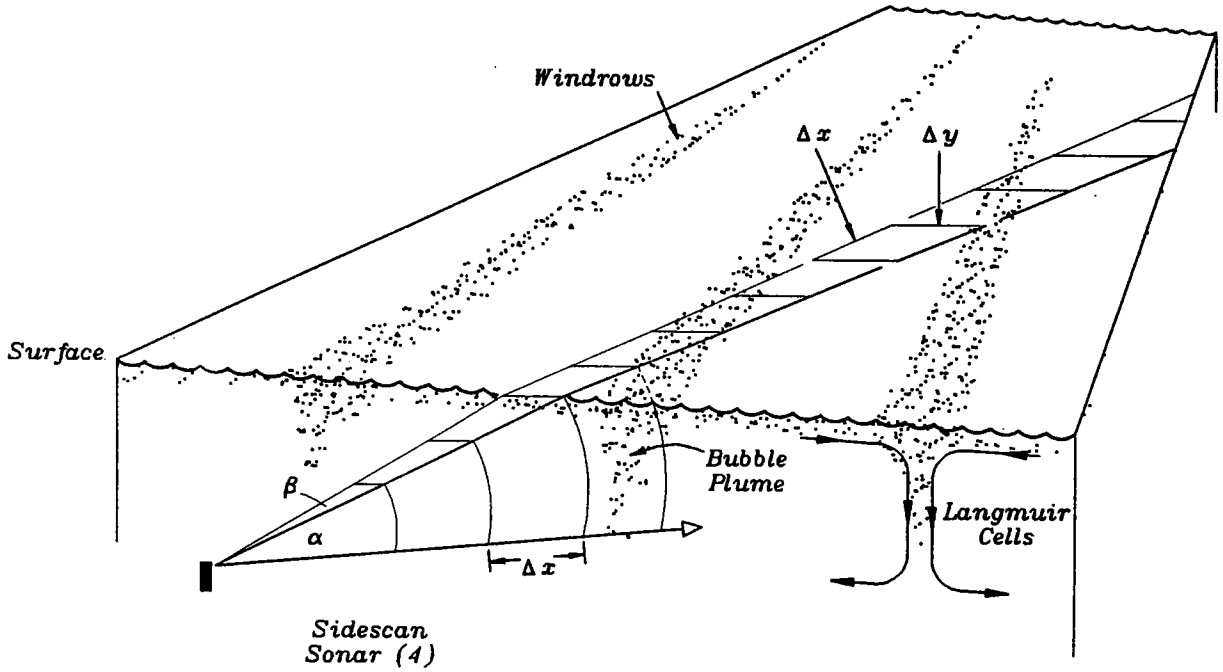

Figure 1 Schematic view of a surface scanning sonar beam with elevation angle α and azimuthal angle β intersecting a near-surface bubble layer which has been organized into windrows by Langmuir circulation. The "footprint" Δx, Δy on the sea surface is determined by the pulse width and the azimuthal beam angle. The inset shows a possible configuration for a four-beam system.

tion will look across rows of bubble clouds collected in successive convergence zones (Figure 1). The backscattered signal intensity will be high in regions where the bubble density is high, providing an image of convergence zone position vs. range and time. The Doppler processing of the same backscattered return will show the convergent velocities themselves. This approach was used by Smith et al. (1987) to detect "low frequency" (0.01 Hz) near-surface velocities and later extended to higher frequencies for the observation of surface wave spectra (Pinkel and Smith, 1987; Smith, 1989). While the sonars developed by Smith and Pinkel were being used from the Research Platform FLIP, Farmer and collaborators from the Institute of Ocean Sciences (Farmer et al., 1990) were pursuing similar measurements from a self-contained package which could be either free-drifting or tethered to a sub-surface mooring (Zedel and Farmer, 1991).

The appeal of the surface-scanning Doppler sonar is its ability to provide a measurement of surface wave directional spectra and at the same time detect coherent features that can be identified with Langmuir circulation. In conjunction with conventional measurements of air-sea fluxes and the vertical structure of density and velocity, the acoustic systems provide information which is critical to improving our understanding of upper ocean dynamics (Price et al., 1987). However, both of the existing systems have limitations. The Scripps Institution of Oceanography (SIO) system, as used on FLIP, is too demanding in terms of size, power consumption, and data storage to be used for an unmanned (i.e. conventional mooring) deployment. The Institute of Ocean Sciences (IOS) system is more compact and can operate as a self-contained, internally recording instrument, but is limited in power and data capacity. This limitation restricts the typical deployment duration to be from tens of hours to a few days, depending on the sample rate used. Some of the IOS sonar deployments have been in a drifting mode, with the instrument suspended at depths ranging from 24 m to 40 m from a small surface float. When free drift is not desired, the instrument requires a dedicated sub- surface mooring. The deployment and recovery of a drifter, or the use of a separate mooring, for the acoustic instrument obviously complicates the logistics and increases the expense of field work.

Our interest is in adapting the surface-scanning sonar technique for making long-term measurements from surface moorings that are already instrumented with a "standard" suite of meteorological and oceanographic sensors. The vision is to develop a fully capable sonar system which introduces no more complexity in the experimental logistics than a current meter.

1.2 Approach

Our long-range goal is to develop a surface-scanning Doppler sonar system optimized for the simultaneous observation of surface wave directional spectra and lower-frequency, near-surface currents. The Doppler capability is necessary to make surface wave observations, and recent results (Plueddemann, et al., in preparation) indicate that Doppler velocity is an important complement to backscattered intensity for the imaging of Langmuir circulation. The instrument would retain the capability to image near-surface bubble clouds using backscattered intensity in the manner of the original Thorpe observations. The design draws on the SIO and IOS sonar systems described above, but modifications

and new developments are implemented with the explicit objectives of extended deployment life, conditional sampling, and real-time data reduction. The operational goal is to develop an instrument that can be routinely deployed for extended periods along with more conventional sensors on a standard oceanographic mooring (cf. Weller, et al., 1990). In addition to longevity, the advantage of such a system is the ability to image the sea surface both directly above (with an upward looking beam) and within a few tens of meters horizontally (with the surface-scanning beams) of the surface and subsurface measurements being made on the mooring.

There are four initial issues to address in adapting existing surface-scanning sonar designs to long-term deployments: Size, power, processing, and storage. These issues are strongly inter-related, and this report is to some extent a study in determining the appropriate compromises to produce an effective instrument. The instrument must be small enough to be deployable in-line on a standard surface mooring. The desired external dimensions are less than 1.5 m in length and 50 cm in diameter. Size considerations effect the operating frequency and beam pattern (through transducer size limitations), and limit the space available for the power source. Battery power must be sufficient for pulse transmission and data processing over the desired deployment period. The goal of the data processing is to reduce the "raw" (i.e. single ping) data stream to a size that will not overflow the mass storage device during a typical deployment. The important processing steps consist of computing surface wave spectra from single-ping data, computing near-surface velocities from data averaged over many wave periods, and applying any necessary corrections (e.g. for platform motion). The maximum storage capacity within the constraints of size and power is desired so that the processing required is kept to a minimum.

The target for instrument longevity will be deployments of 6 to 10 months. It is evident that unless the raw acoustic returns are processed prior to recording, data storage, rather than the power budget, will be the limiting factor. Thus, a primary thrust of the development must be the implementation of robust processing algorithms to reduce the high-frequency data by computing higher-order products such as covariance matrices and spectra. This is a major departure from existing systems where raw data is recorded and post-processing is done aboard ship (e.g. Pinkel and Smith, 1987) or in the lab (Zedel and Farmer, 1991). Even with the use of real-time processing, it will not be feasible to collect data continuously. The total amount of data will initially be limited by time-conditional sampling (e.g. one 15 minute measurement interval every 2 hours), but could later be extended to intensity-based or velocity-based conditionals (e.g. use acoustic intensity to estimate wind speed and begin sampling at a wind threshold).

In addition to the design constraints resulting from extended deployment duration, use of a surface-scanning sonar on a surface mooring raises the issue of platform motion. Preliminary results from a surface mooring in the North Atlantic indicate that an instrument at 30 m to 50 m depth would experience low frequency (minutes to hours) tilts of only a few degrees, and high-frequency (seconds to minutes) variability of less than 5 degrees. The surface-scan technique has been used successfully under similar conditions (Pinkel and Smith, 1987). Of more concern is azimuthal variability. Measurements from the same mooring indicate that rms high-frequency heading variability may be consistently in the

range of 10 to 30 degrees. These variations are large enough to present difficulties in observing Langmuir circulation detecting high-frequency surface waves at large distances from the sensor. Our approach to the mooring motion problem is to design for a low-power, high-frequency motion sensing package to be included in the sonar system. In the interim, analysis of data from a motion package soon to be deployed will improve our knowledge of surface mooring motion and allow us to evaluate expected instrument performance. If deemed feasible, modifications to the packaging (e.g. reduce drag and asymmetry) and the processing (e.g. incorporate motion correction in real-time) could be made to facilitate the transition from sub-surface to surface mooring deployment.

Once the general design criteria have been evaluated, the detailed design specifications can be drawn up. This report describes specifications for the principal electrical and mechanical components of a multi- channel, surface-scanning Doppler sonar. These components can be grouped into five principal sub-systems: The analog front-end, the controller, the digital signal processor, mass storage, and power circuitry. The report stops short of describing the associated software components of the sonar system which would include signal generation and control, data management, and data processing routines.

2.0 System Parameter Analysis

In this section of the report the selection of system operation parameters is explored. These parameters include the frequency of operation, signal duration and type, required source level, transducer beamwidth and many others. Of prime importance for this instrument is maximizing resolution while maintaining a low-variance estimate of the Doppler velocity in any given range cell. However, these are competing issues because the velocity variance is improved with increasing pulse duration while resolution decreases. Careful analysis of trade-offs in the selection of frequency and signal duration are required in order to make a final selection for a particular application. On this issue and many others we are aided by the work of Smith (1989) which describes the design of an optimum Doppler sonar system for surface use. These results are drawn upon in order to carry out the design of a self-contained instrument for use on an ocean mooring.

2.1 Transducer & Signals

The parameters of the transducer and the signals used to drive it determine the fundamental capabilities of the system and must be chosen with care. The beampattern, array size, peak power output, receive sensitivity, efficiency and many others are all important. As with other portions of this system there are many competing requirements in the selection of transducers for a sonar capable of Langmuir circulation and wave spectra measurements. Some of these considerations are outlined below.

Frequency selection is dependent on desired range and the minimum signal to noise ratio (SNR) required for processing the signal. SNR depends on the attenuation due to absorption and spreading, the source level, the receive sensitivity, the array directivity and the ambient noise level. Attenuation increases monotonically with increasing frequency. For our application, a maximum range of 400-600 m was desired, ruling out frequencies above about 500 kHz due to excessive attenuation and spreading losses. Frequencies below about 100 kHz would result in an unacceptably large transducer due to the trade-off between frequency and array size for the desired beam pattern (see below). Ambient noise decreases as frequency increases and reaches a minimum at about 200 kHz before increasing again with thermal noise. Thus, the frequencies between 100 kHz and 300 kHz were considered in the design study.

In order to benefit from the surface-scanning technique, the transmitted beam must be narrow in azimuth and broad in elevation. For an expected deployment depth of 30 m, simple geometry allows determination of the elevation angles necessary to intersect the surface at the minimum and maximum desired ranges. Specular reflection of sidelobe energy from the sea surface corrupts the ranges nearest the sonar, restricting the minimum range for good surface-scan returns to about 50 m horizontally from the transducer. Ideally, a maximum range of about 1 km would be used to resolve several cycles of large-wavelength swell and Langmuir cells with convergence-zone spacing of order the mixed layer depth. The maximum range of 600 m used in this design study is a more realistic objective given the constraints of transmission losses and transducer size discussed above. Thus, elevation angles were estimated for a beam which would intersect the surface at 50 m and 600 m

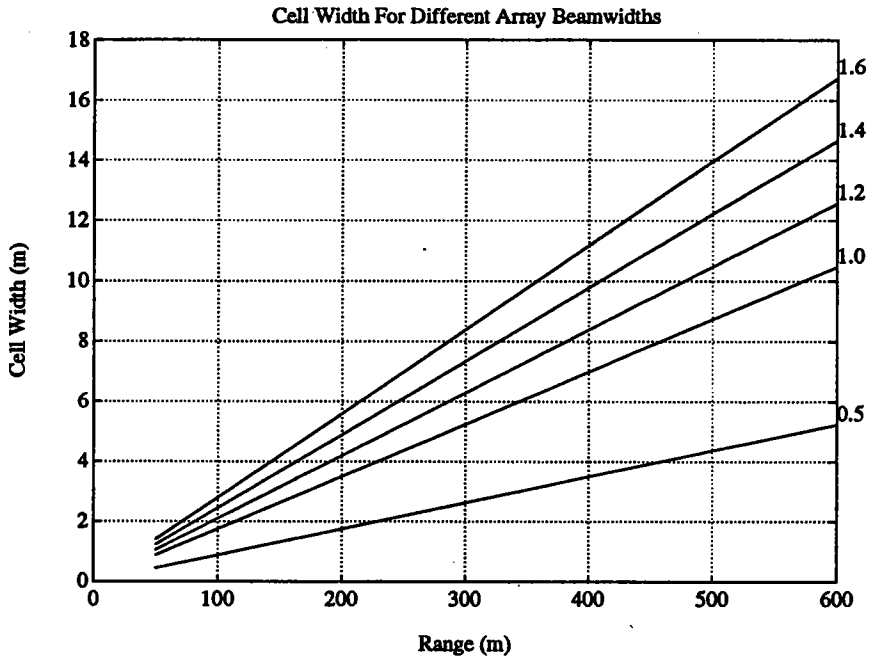

Figure 2 Width of a volume cell for different transducer beamwidths showing the difficulty in maintaining a small cell at maximum range.

with the transducer at 30 m depth. The resulting dimension of the beam in elevation is 24 degrees and the centerline of the beam would be pointed at an angle of +14 degrees from the horizontal.

The horizontal resolution of the sample volume is controlled by the duration of the transmitted pulse and the azimuthal extent of the beam pattern. A very narrow beam azimuth is required to produce the desired resolution of between 2 m and 10 m in the across-beam direction. The width of the sample cell at different ranges for various transducer beamwidths is shown in Figure 2. Between 100 m and 500 m the resolution of a 1.4 degree beam would vary between about 2 m and 12 m, reasonably close to the desired values. Picking the cell width at the midway point in range (250 m) as a reference, it is seen that a beamwidth of 1.4 degrees could be characterized by an azimuthal resolution of 6 m.

A very narrow beam requires a long array which may be impractical for an instrument on a mooring cable. Physical constraints dictate that the transducer array length be much less than a meter since the long axis must be mounted horizontally on the mooring. The target size for the transducer dimension is 50 cm. Array dimension with respect to operating frequency and beamwidth is shown in Figure 3. Size constraints immediately rule out a 100 kHz operating frequency for any beamwidth less than about 1.5 degrees. Appropriately sized arrays for frequencies of either 200 or 300 kHz are possible for beamwidths down to about 0.8 degrees. A 1.4 degree beam at 200 kHz results in an array size just over 30 cm, which is well within the design constraints.

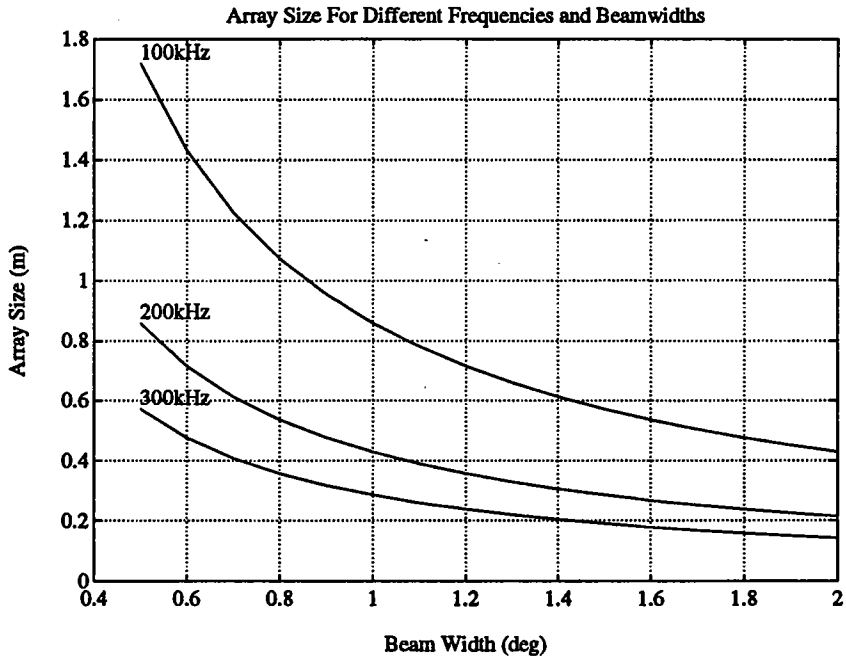

Figure 3 Array size for different horizontal beamwidths. Note that for a 0.5 degree beam at 200 kHz a transducer almost one meter long is required.

Directivity increases as the beam is narrowed. Thus a highly directive pattern is desirable in order to increase range. However, as discussed above, the narrower the beam the larger the transducer. The directivity attained with different vertical and horizontal beamwidths is shown in Figure 4. The expectation for a beam pattern with X (elevation) and Y (azimuth) beamwidths of 25 by 1.4 degrees would be about 30 dB.

2.1.1 Maximum Attainable Source Level

Maximum source level is function of limits imposed by cavitation and shock, the point beyond which the signal goes non-linear. In order to maximize range and signal to noise ratio the highest source level possible should be used in the system. An expression for the cavitation limit is given by

$$S_c = 284\text{dB} + 20\log P_c - 20\log f - 20\log(\theta\phi) \tag{1}$$

where

$$P_c = 1 + \frac{d}{10} + \left(\frac{f}{36kHz}\right)^2 \tag{2}$$

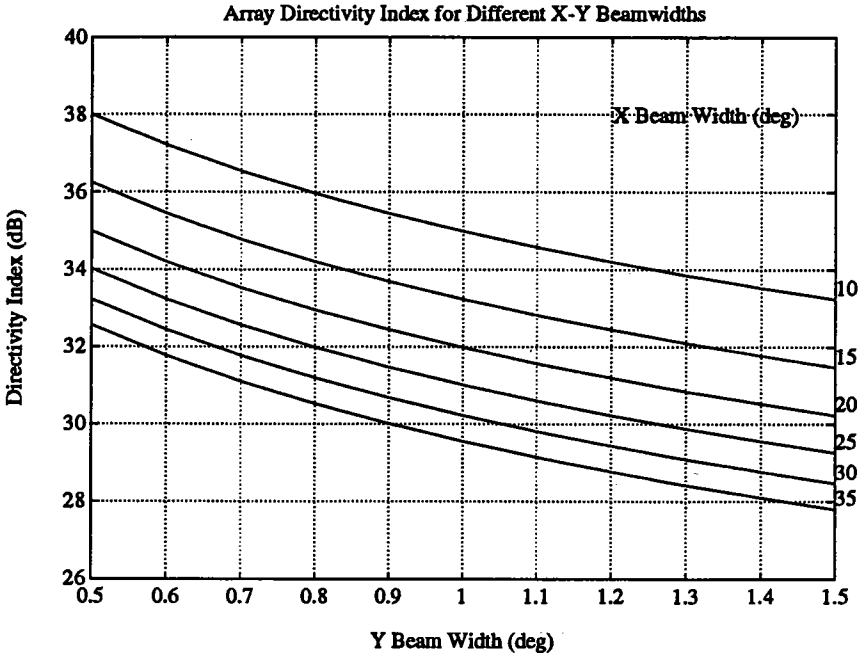

Figure 4 Directivity index for different size arrays. The narrower the beam, the more gain. For 1.4 by 25 degrees the DI is about 29.5 dB. A 0.5 degree by 25 degree beam has a 4 dB greater directivity index.

d is the depth, θ and ϕ are the transducer beamwidths in radians and f is frequency (Smith, 1989). For the ranges of transducer sizes and frequencies considered here the cavitation limit for the source is close to 250 dB, which is greater than the limits imposed by shock.

The saturation limit is somewhat more difficult to compute, but has been calculated by Smith for a 30 by 2/3 degree beam and plotted with respect to frequency (Smith 1989, Fig

7), reproduced here as Figure 5. The figure shows that at 200 kHz the source level limit imposed by saturation and shock is about 225 dB. This is approximately the maximum level attainable given electronics capable of driving the transducer with enough power.

Electrical power required is a function of amplifier and transducer efficiency. Electrical power may be computed from

$$P = \frac{1}{E_T E_A} 10^{\frac{(SL - 170.8)}{10}} \tag{3}$$

where SL is the desired source level in dB re μPa at 1m, E_T is the efficiency of the transducer and E_A is the efficiency of the amplifier. For a class B amplifier E_A is at most 87%. Efficiency for sidescan-type transducers is on the order of 40% depending on size and construction. It is estimated that approximately 1200 W will be required to produce the desired source level of about 225 dB with a 24 by 1.4 degree transducer.

2.1.2 Sonar Equations: Estimated SNR

The losses in the system include the attenuation and spreading loss, the target backscatter strength and the area of the surface which is insonified. An expression for the total loss in dB is given by

$$\text{Loss} = S_s - 2\alpha r - 40\log r + 10\log(r\phi\Delta R) \tag{4}$$

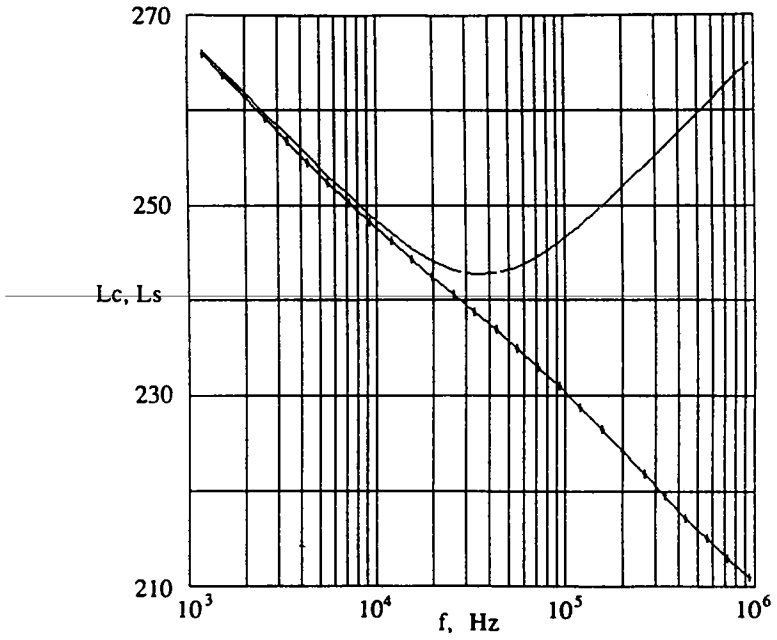

Figure 5 Saturation limit with respect to frequency plot reproduced from Smith (1989) with permission of the American Meteorological Society.

from Smith, 1989. S_s is the scattering strength, $2\alpha r$ is the two-way attenuation, $40\log r$ is the loss due to the round-trip spreading, and the term $r\phi\Delta R$ is approximately the surface area illuminated by the beam. Attenuation and spreading losses dominate as shown in Figure 6. The backscatter strength $10\log(r\phi\Delta R)$ for a different beamwidths and pulse durations is shown in Figure 7. Total round-trip losses which include the signal return from the subsurface bubble cloud may be calculated from equation (4), however the scattering strength term S_s must be determined in order to apply the equation.

It is possible to estimate the required dynamic range for the sampling system by examining the total losses due to attenuation and spreading over the signal path. At 200 kHz the difference in loss between 50 and 500 meters is about 80 dB. This is the approximate difference in expected signal strength from the closest sampled range bin to the farthest. The actual absolute magnitude of the signals depends on the scattering strength which is a function of the bubble density. The variation of signal strength with respect to range (or time) requires a sampling system with a very wide dynamic range or with time varying gain (TVG) in order to keep the signal magnitudes within range of the analog to digital converter. A 16-bit A/D converter gives a theoretical dynamic range of 96 dB, but limits the instantaneous dynamic range at either end. Some sort of programmable gain control is usually used in these types of sonar systems, and the particular method selected for this implementation is discussed further in a later section.

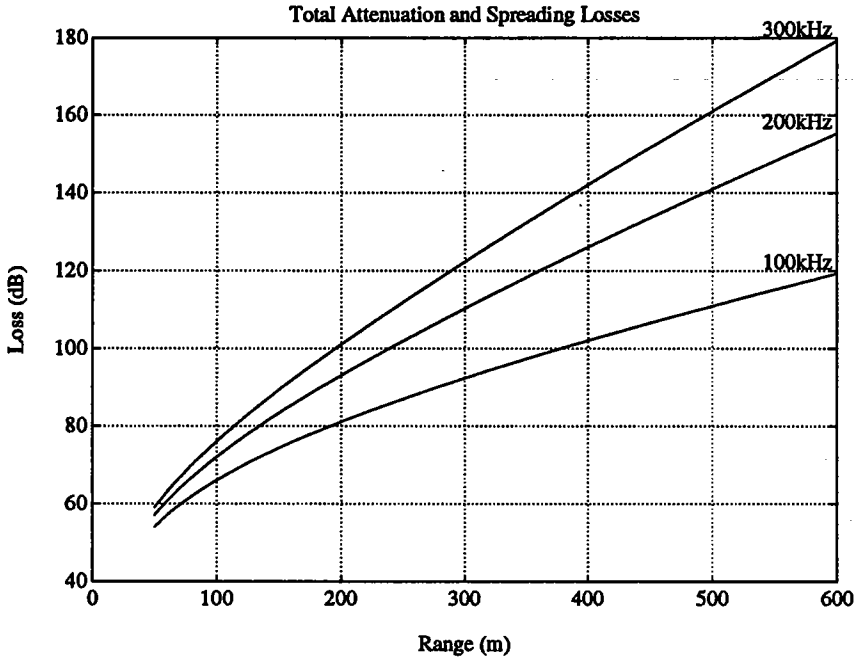

Figure 6 Sum of the attenuation and spreading terms in equation (4).

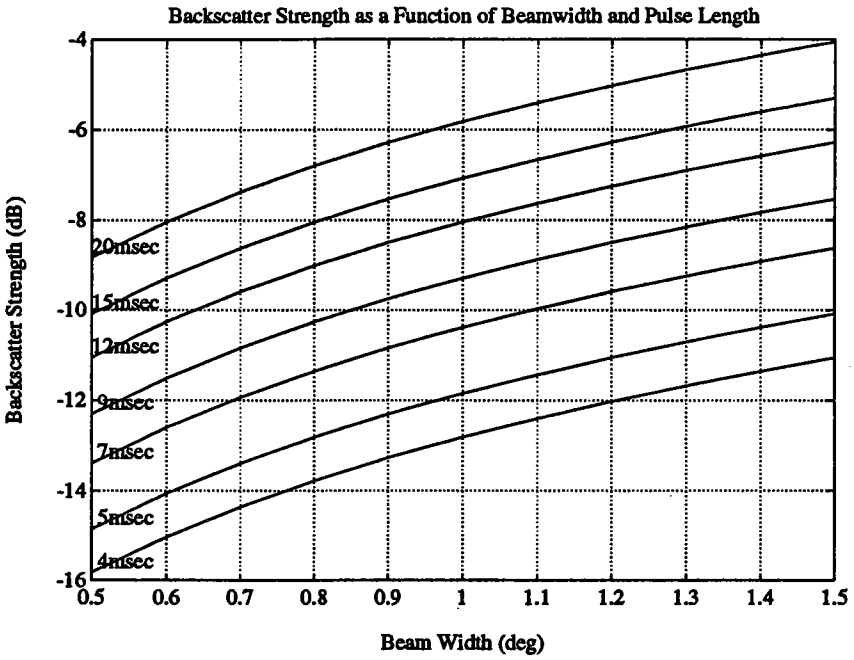

Figure 7 Backscatter strength as a function of beamwidth and pulse duration. As expected, the greater the surface area and the longer the pulse, the greater the backscatter strength.

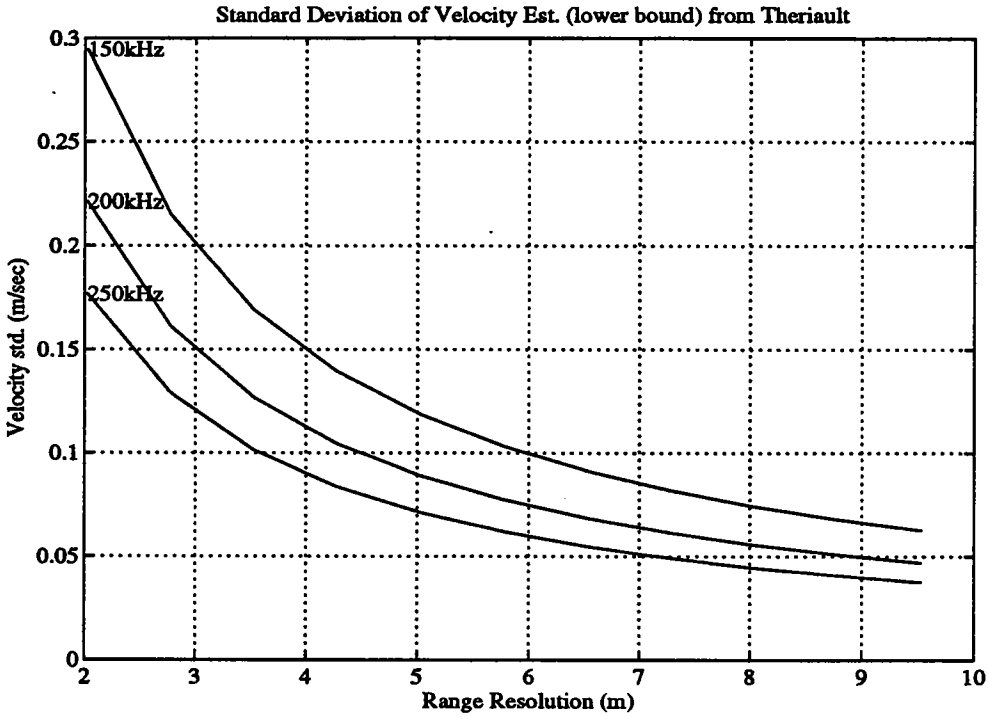

Figure 8 Curves of the standard deviation of the velocity estimate from 150 to 250 kHz and 2 to 10 m range resolution (2.7 msec to 13.3 msec pulse lengths).

2.2 Velocity Estimation

The velocity measurement is the principal observable of the system, and the required velocity precision puts constraints on many system parameters including pulse duration, frequency and the number of estimates that must be averaged together. The Doppler velocity estimate from the backscattered acoustic energy in a given range cell is obtained using the complex covariance method (Miller and Rochwarger, 1972). For a transmission consisting of a simple gated pulse, the lower bound on single-ping standard deviation of the Doppler estimate is given by

$$\sigma = \frac{c}{4\pi f T} \tag{5}$$

where c is the speed of sound, f is the center frequency, and T is the pulse duration (Theriault, 1986). Range resolution for a given pulse duration is

$$L = \frac{cT}{2} \tag{6}$$

The desired range resolution of 2 to 10 m constrains the possible pulse durations to approximately 3 to 13 msec. A plot of equation (5) from 150 to 250 kHz for range resolution of 2 to 10 m is shown in Figure 8. It should be recognized that equation (5) is a lower

bound, and in actual practice is never achieved. A factor of 1.4 has been suggested for use in converting the lower bound to an operational standard deviation estimate (Brumley, et. al., 1991). Other authors have suggested factors between 1.5 and 3.0. Irrespective of the correction factor, Figure 8 is useful in the relative comparison of velocity precision for different pulse durations and frequencies.

The desired standard deviation of the velocity estimate depends on what aspect of upper ocean dynamics is under study. The design goals for the instrument are for detection of both surface waves and Langmuir circulation. Local wind driven seas and swell from distant storms encompass wave periods from about 5 to 15 s and have associated orbital velocities of about 8 to 23 m/s. A velocity estimate standard deviation near 1 m/s is adequate to detect these waves. However, since a sampling rate of order 1 Hz is also required, the ping repetition rate of the sonar must be considered. With a desired maximum range of 600 m, the sonar has a minimum pulse repetition time of 0.8 s, sufficient for surface wave detection if the desired velocity precision can be obtained from a single ping. Figure 8 shows that even for the shortest pulse durations considered the single ping velocity precision is adequate for the detection of surface waves.

Detecting velocities associated with Langmuir circulation is more difficult. The convergent velocities in Langmuir cells vary with the size of the cell. Observations suggest that typical velocities are between 5 and 20 cm/s. A velocity precision of about 1 cm/s is desirable for the detection of these velocities. Clearly, at short time scales these signals will be overwhelmed by the orbital velocities of the surface waves. However, Langmuir circulation is long-lived compared to the period of a wave and given a sufficient "dwell time" the orbital velocities can be averaged out. Figure 8 shows that a minimum dwell time is also needed to reduce the velocity standard deviation, since the single-ping standard deviation is significantly greater than 1 cm/s even for the longest pulse duration considered.

The standard deviation of the velocity estimate is reduced by a factor of $1/\sqrt{n}$ by averaging over n pings. Of immediate interest is the number of pings required to achieve a 1 cm/s standard deviation. This may be estimated after a frequency and pulse duration are determined. For the moment we will consider a operating frequency of 200 kHz and a range resolution of 5 m, resulting in a pulse duration of 6.7 msec. Figure 8 shows that the single-ping standard deviation for these operating parameters is about 10 cm/s. To reduce this by a factor of 10 requires at least 100 pings. In order to account for the difference between the lower bound standard deviation and typical observed standard deviation this may need to be increased to 200 or 300 pings, or a total dwell time of 2-3 minutes with a ping repetition time of 0.8 s.

One of the problems on a moving mooring is maintaining the sonar beam in a single direction of look (plus or minus the beamwidth) during the time needed to record 100 or more pings. Since the likelihood of an instrument located about 30 meters below a surface mooring moving only a few degrees over several minutes is rather low, it is desirable to reduce the number of pings required to obtain a given velocity precision. This drives us to the consideration of coded signals to decrease the single-ping standard deviation of the velocity estimate.

2.2.1 Velocity Estimates Using Coded Waveforms

Coded waveforms have been proposed and used by a number of investigators including Brumley, et. al. (1991) and Pinkel and Smith (1992). Any new instrument must be designed with the capability to generate and process coded waveforms so as to efficiently use battery power and minimize the amount of time required to make Langmuir circulation measurements.

Brumley, et. al. developed their coding technique to reduce the variance of an acoustic Doppler current profiler (ADCP), which is primarily used in applications involving volumetric (rather than surface) backscatter. Pinkel and Smith, whose work is focussed on tracers near the surface, developed what they call repeat-sequence coding for improving Doppler estimates for studies of Langmuir circulation and measurements of wave spectra. The two methods are similar but were developed independently.

Coded pulses are usually phase shifted signals with the size of a given phase-encoded digit determined by the bandwidth of the transducer. Use of coded waveforms means that the signal generation hardware must be capable of producing phase shifted signals, and that the amplifier-transducer combination must have a bandwidth larger than one over the digit length. At a center frequency of 200 kHz, approximately 10-20 kHz of bandwidth is available depending on the transducer. A 10 kHz bandwidth signal means that each code digit can be 100 usec long, and a 4 msec pulse then has 40 digits.

The expected gain available through use of coded signals depends on a number of factors, including bandwidth and code length, though generally overall performance increases with the code length (Pinkel and Smith, 1992). Pinkel and Smith found that all doppler measurements were enhanced through use of coded signals, and thus the capability to generate these signals is included in this design, and system bandwidth is maximized in order to generate signals with many digits.

2.3 Summary of System Specifications

Using the exploration of parameters in the previous sections as a guide, a set of system specifications can be put together in order to meet the design goals. The principal parameters chosen on the basis of this study are shown in Figure 9 and described briefly below.

The principal constraint on the system is to maintain high spatial resolution while maximizing the velocity precision for each ping. Given this constraint, we want the highest operating frequency which can be expected to reach 600 m range before SNR becomes unacceptably low. Consistent with the conclusions of Smith (1989), a 200 kHz operating frequency is chosen. The bandwidth of 10 kHz allows the use of coded transmissions. Geometrical considerations for a transducer at 30 m depth determine the 1.4 degree by 24 degree beamwidth which will give an azimuthal resolution of 2 m and 12 m at ranges of 100 and 500 m, respectively. Note that at 200 kHz the transducer array necessary to generate the 1.4 degree azimuthal beam is reasonably sized (about 30 cm in length). We anticipate that the final configuration would include four beams separated by 45 degrees in

Table of System Specifications

Basic Parameters	
Operating frequency	200 kHz
System bandwidth	10 kHz (min)
Beam width (azimuth)	1.4 degrees
Beam width (elevation)	24 degrees
Beam separation (4 beam array)	45 deg. azimuth
Power level (peak)	225 dB
Signal type	programmable
Deployment depth	30 m
Maximum range	600 m
Azimuthal resolution	6 m at 250 m range
Pulse duration (uncoded)	5-8 msec.
Range resolution (uncoded pulse)	4-6 m
Single ping velocity precision (uncoded pulse)	0.10 m/s
Bit time for coded pulse	100 usec (min)
Pulse repetition time	0.8 sec
Hardware Parameters	
Digitizer resolution	16 bits
Fine gain control range (TVG)	40 dB
Coarse gain control range	30 dB
Digitizer sample rate (min)	20 kHz per Channel
Battery capacity (max)	10 K W-H (lithium)
Storage capacity	500 Mbytes

Figure 9 Summary of preliminary system specifications for the instrument.

azimuth to allow directional estimates to be obtained from the surface wave data and to ensure that one beam will be pointed nearly cross-wind at any time for the detection of Langmuir circulation (Figure 1, inset). Considering the case of uncoded pulses as a baseline, we see that a pulse duration of 6.7 msec would result in a range resolution of 5 m (matched to the azimuthal resolution at approximately mid-range) and a single ping velocity precision of about 0.1 m/s. It is recognized that the actual velocity precision will not be as good as this lower-bound estimate, and coded pulses may be necessary to reduce the velocity variance while maintaining the range resolution. A pulse repetition rate of 0.8 msec is the minimum interval which will still allow a maximum range of 600 m.

2.4 Sampling Strategies

With the basic system parameters determined, it is possible to review the sampling strategies necessary to achieve the goal of extended deployment life. A variety of methods are available for data reduction, which will essentially involve incorporating post-processing techniques similar to those used by Zedel and Farmer (1991), Pinkel and Smith (1987), and Smith (1991) into the on-board system electronics. Modern, low-power microprocessors are capable of these tasks, and small, rugged mass storage devices capable of recording hundreds of megabytes of data are available for use in oceanographic instrumentation. Thus, we expect that data processing and storage sufficient to meet the design goals, while not a trivial task, can be successfully accomplished, and that instrument deployment life will be power limited. Indeed, a simple calculation using a 1200 W power amplifier and a 5 W electronics package, coupled with a 10 kW-hr battery capacity shows that a maximum of about 700,000 pulse repetitions can be made on each of four transducers before the battery power is exhausted. With a pulse repetition time of 0.8 s, this limits continuous operation to about 160 hr. Clearly a sampling strategy which reduces the total power drain must be implemented.

From Section 2.2, above, we determined that a minimum of about 100 pings would be required to make one "measurement", where a measurement is defined as a sequence of pings with sufficient velocity precision to observe Langmuir circulation. The maximum number of pings to be averaged together for one measurement is limited by the time scale for change in the phenomenon being observed. We would like to average no more than about 30 min of data (2000 pings) in a single measurement. Figure 10 breaks down the total pings available for a given system configuration and battery capacity by presenting the deployment lifetime as a function of the number of measurements per day for several choices of the number of pings per measurement. Using the minimum acceptable value of 100 pings per measurement, a 9 month deployment life can be achieved if measurements are made once per hour. Increasing the pings per measurement to 1000 improves velocity precision, but the measurement rate is restricted to 4 per day for a 6 month deployment. This again leads us to consider the benefits of coded pulses. Reducing the number of pings necessary to obtain acceptable velocity precision will allow more measurements per day for a given deployment life.

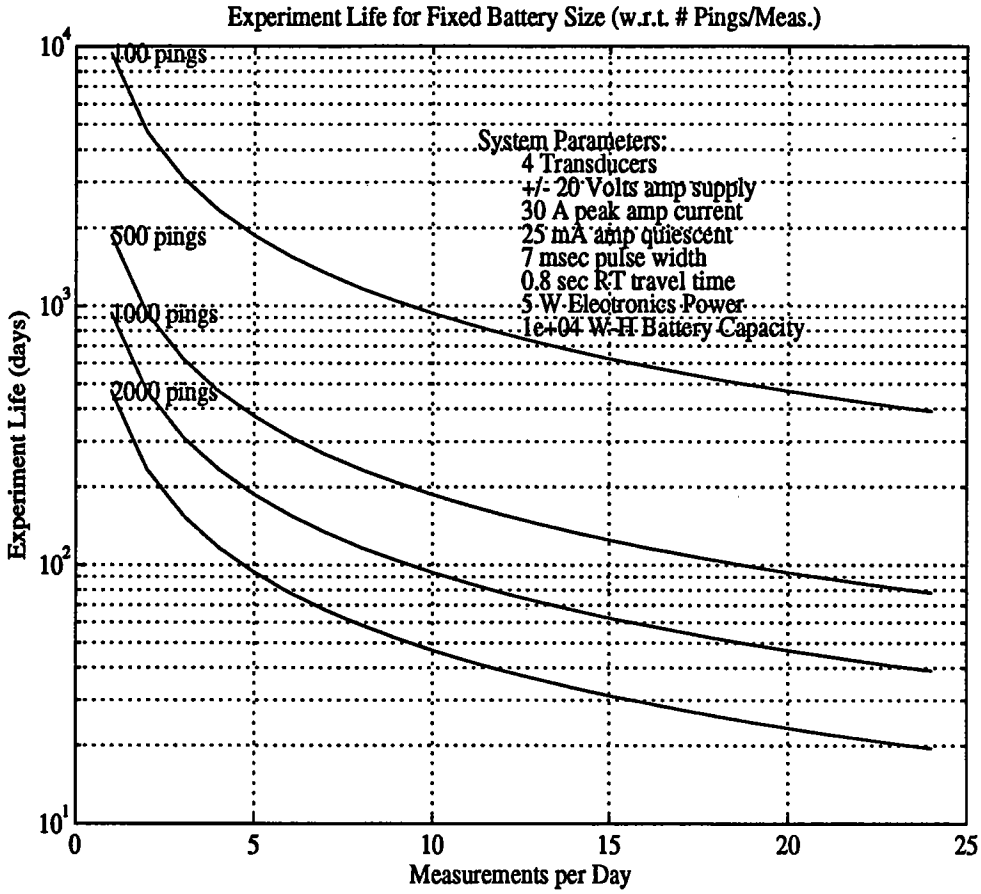

Figure 10 Deployment lifetime vs. number of measurements per day for 100-2000 pings per measurement. The deployment lifetime is estimated based on the system parameters shown in the inset.

3.0 Impact of Mooring Motion on the Instrument

Yaw (change of heading) of the instrument as measurements are being made causes different parts of the advecting bubble field to be sampled. High frequency changes such as those expected on an instrument 30 meters below a surface mooring may make it difficult to insonify the same region with consecutive pings. Expected variability of the surface mooring heading may be 10 to 30 degrees on time scales of a few seconds.

The most basic concern about heading is that the orientation of the transducer not change more than about half its beamwidth during the round trip travel time. If this condition is not satisfied the system will not work at all as proposed, and active beam steering will be needed in conjunction with high-frequency measurements of angular velocity and acceleration. In the discussion below it is assumed that the rotation during each ping is small, so that the problems are restricted to the ping-to-ping rotations.

3.1 Impact on Directional Wave Spectra

It has been shown that a surface wave orbital velocities can be estimated from single ping sonar data. Thus, with the assumption that azimuthal variability is small (some fraction of the beam width) during the pulse transmission and reception, the impact on surface wave measurement is reduced to the problem of determining the underlying wavenumber frequency spectrum from a series of "snapshots" (pings) which may have significantly different orientation. Smith's most recent Langmuir circulation paper (Smith, 1992) hints that variations in azimuth may be accounted for in the spectral estimator (although no references are cited and it is indicated that this is work in progress). Given that many high-variance Doppler/range measurements can be combined over time, it appears as though it will be possible to estimate directional spectra from single-ping Doppler data and accurate heading information. Thus it may be that heading variability will not adversely impact wave spectra measurements.

3.2 Impact on Sidescan Intensity Measurements

We assume that sidescan intensity measurements adequate for detection of Langmuir circulation convergence zones are obtainable from single pings. Thus, similar to the surface wave measurements, the problem reduces to "mapping" successive pings with different observation angles to a useful space/time grid. Zedel and Farmer (1991) have used heading information to project the sidescan intensity measurements of bubble clouds onto a composite map. They appear to have used un-averaged or single-ping data in this analysis, though this is not clear in the paper (see pages 8895-8896). However, in order to make the projection, the motion of the instrument had to be estimated relative to the advecting surface layer. This was done with a current meter located below the instrument package. Assuming that on the mooring the x-y movement of the instrument could be measured, the same procedure could be applied in the proposed instrument. A major difference between the Zedel-Farmer experiment and the operation of a similar device below a surface mooring is the angular velocity that might be encountered on the moored instrument. Slow

changes in heading will sweep the beam across the bubble field and allow some averaging as beams are overlaid in the projection process. There may be little overlap on a quickly rotating platform (moving at the maximum rate of about half a beamwidth per ping), and the resulting composite map may be not nearly as good as that attained by Farmer's instrument.

3.3 Impact on Doppler Measurements for Langmuir Circulation

A velocity variance of about 1 cm/s is required for making Doppler-range images that will show the formation of Langmuir circulation (such as in Smith, 1992, figure 7, color plate). Given the range resolution desired, it is unlikely that the single-ping variance can be reduced much below 8 to 10 cm/s. Even with 4-bit repeat sequence codes, Smith only claims single ping variance of 10 cm/s for his data from SWAPP, and averages 80 pings together to reduce the variance to about 1 cm/s. Thus a minimum averaging time, or dwell time, of about one minute will probably be required. Smith's data was taken from Flip, where a 3 degree RMS heading variation was maintained. On a surface mooring heading variability will be significantly larger, with a time scale of variation on the order of the dominant surface wave period (i.e. several seconds). Thus, unlike the situation for surface waves or sidescan intensity, the dwell time required to make a Langmuir circulation measurement is long compared to the time scale for variation in heading. We expect that it will be difficult to make Doppler measurements accurate enough to detect Langmuir circulation from an instrument mounted on a surface mooring without using some sort of heading compensation.

Even if the mooring was stable enough to allow one minute averages to be made (say from a subsurface mooring), over 1500 to 2000 pings the instrument heading will almost certainly change. This will make Doppler images such as those made by Smith difficult to interpret. A possible solution for this particular problem (slow enough rotation so as to allow 1 minute averages, yet steady heading changes over 20 or so minutes) is to apply a projection to the data in order to make a map similar to that done by Zedel and Farmer for sidescan intensity images. Additional investigations will have to be done, but this may allow successful operation from at least a subsurface mooring.

Zedel and Farmer made Doppler measurements with a vertical sonar and encountered exactly the problem described here (Zedel and Farmer, 1991). Their solution was to make only a "representative average" by combining similar profiles through a conditional averaging scheme. A representative average over many cells (e.g. figure 11 of Zedel and Farmer) is useful, although not as interesting as being able to distinguish the time-evolution of individual cell patterns as done by Smith. Zedel and Farmer matched vertical velocity profiles based on bubble penetration depth, with the latter presumably determined from the backscattered intensity. A similar intensity-based averaging scheme could be used to make a representative average of horizontal velocities from surface-scanning sonar data. However, it is not clear that this technique will work as well with a surface-scanning sonar as it did for the vertical sonar.

3.4 Motion Compensation

There are two ways to compensate for the changes in heading that the system will observe: Mechanical steering and electrical beamforming.

Beamforming is very attractive because it requires no moving parts and allows corrections and processing to all be done in software. However, the hardware required to steer the transmit beam and to also steer the receive beams is both complex and power hungry. In order to steer the transmit beam in the desired look direction each element of the transducer must be driven with a time-delayed signal. This requires as many amplifiers and sets of drive electronics as there are transducer elements. While the construction of such a system is not impossible, particularly since each individual transducer is driven at a lower power level than a single large element, the total parts count is high. Likewise at the receive side, each individual element must have a complete analog front-end and its data must also be digitized and then processed. The total increase in complexity is at least a factor of 8, and might be as high as 16 or 32, depending on the desired beam-pattern and resolution. Thus this solution will not be considered further here, though it is possible that as size and power for integrated circuits decreases this may become feasible.

A much simpler method would use mechanical steering. This is not complicated, particularly for a shallow application, and similar mechanical systems are used in scanning sonars and some mechanical releases. A mechanically steered transducer head would be rotated using a stepper motor with feedback provided by a compass inside the sensor module. The requirement is to hold the heading within about three degrees, which should be possible, depending on the speed of rotation. A simple control loop is run by the internal computer to provide smooth steering and avoid oscillation of the stepper motor under calm conditions. Of greatest concern is the power consumption of such a system, and the noise that it might introduce into the acoustics. Both of these concerns can be taken care of by only moving the head between pings and maintaining the stepper motor drive electronics in a quiescent state otherwise. If the motors only draw current while switching, the total power consumption of the steering unit will be small. Of more concern is the time needed to move the head a few degrees. This time must be short in order to keep the pings as close together as possible.

The mechanical steering method needs to be investigated in more detail, but it may be the best way to get around the problems of yaw in the surface scanning sonar.

4.0 Electrical And Mechanical Systems

Based on the work of the preceding section an actual implementation is proposed. This implementation is discussed below in detail.

4.1 System Operation

The system will remain in a low-power state most of the time, becoming active at scheduled intervals. Surface wave periods, time scales for evolution and decay of Langmuir circulation patterns, and requirements for the reduction of Doppler velocity variance indicate that a desirable sampling strategy would be approximately 750 pings (a 5 minute measurement interval) every four hours.

When sampling begins the transmitter pings on all four transducers simultaneously with a short coded tone burst approximately 5 msec long. The transducer is switched from transmit to receive, and the four-channel analog front-end filters, demodulates, amplifies and digitizes the acoustic return. Storage of the incoming data in signal processor memory is accomplished in the background with very little overhead. During each collection period the processor is working to reduce the previous ping's data to Doppler estimates at all range cells on all four beams. Estimation of Doppler velocity is done using the complex covariance method (Miller and Rochwarger, 1972) which may be efficiently implemented using the auto-correlation function. In addition to Doppler estimation the energy in the received acoustic return is processed to yield side scan data. This amplitude-range data is stored for further processing into sonograms for visual interpretation. The data is reduced into a compact form for efficient disk storage.

The Doppler data is accumulated over many pings, for example 5 minutes of sampling at 0.8 seconds each yields 750 Doppler-range measurements on all four channels. This data is then used to estimate sea surface spectrum which is then stored in lieu of the raw Doppler data. Depending on experiment length some raw data may also be stored. Storage of raw data is a programmable parameter which may be set by the user prior to deployment. After the collection and processing sequence is complete, the data is stored to disk and the system returns to a low power state to await the next sampling cycle.

4.2 Doppler Sonar System Description

Components of the system include the side-scan transducers, power amplifier, analog front-end, digital signal processing (DSP) system and mass storage subsystem for archiving data.

4.2.1 Mechanical Layout and Transducers

The target length for the electronics package is approximately 2 feet, and batteries will occupy approximately 5 inches per kilowatt-hour of energy (in the form of lithium DD cells) in a six inch diameter pressure case. Depending on operational requirements up to 4 feet

of pressure case for battery storage could be used to obtain a battery capacity of about 10 kW-h. Thus, a pressure case sufficient for housing the electronics and the maximum battery capacity would be about 6 feet long. The system will be designed for four sidescan transducers with beams oriented 45 degrees apart in azimuth. The dimensions of the sidescan transducers for generating a 1.4 by 24 degree beam are 2.5 by 1.5 by 13 inches long. These will have polyurethane faces and will be contained in aluminum housings for operation within 100 meters of the surface. Housed in a load-bearing, protective cage for deployment in-line on a mooring, the sonar system would be approximately 9 feet long by 18 inches wide (Figure 11).

4.2.2 Electronics Systems

The electronics systems for the Doppler Sonar include a system controller, digital signal processor, analog processing circuitry as well as disk storage for the data (Figure 12).

Overall system control is maintained by the CPU, here a miniature DOS-based computer which does all high-level control and coordinates data collection and processing. The other subsystems can be shut off in order to save power when they are not being used, the controller can shut itself down or go into a very low power state to await the next data collection period. In this preliminary design the PC-104 form-factor has been selected for the CPU and the other boards in the system. The size is very compact, only 3.8 by 3.6 inches and the cards stack together to form a very space-efficient package.

The sonar signal is generated by digital hardware controlled by the CPU. The phase coded transmit signal is created from a common clock at the carrier frequency that is phase switched 180 degrees according to the binary code word. The coded signal is then fed to the four power amplifiers and side-scan transducers. The power amplifier is designed to be highly efficient and matched to the digital signals. Efficiency is very important due to the high power needed to attain low-variance Doppler estimates at maximum range while also allowing instrument longevity with a limited battery supply.

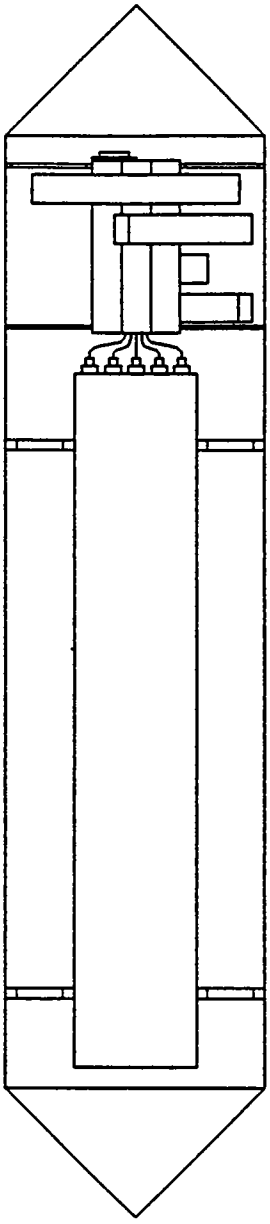

Moored Instrument
Side View

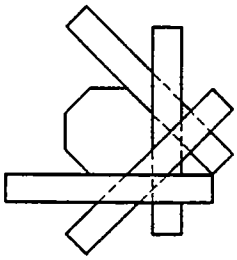

Transponder Array
Top View

Figure 11 Schematic depiction of the surface-scanning sonar configured for deployment on a mooring. A four-beam transducer array and an electronics module would be housed in a load cage and deployed in-line at approximately 30 m depth on the mooring.

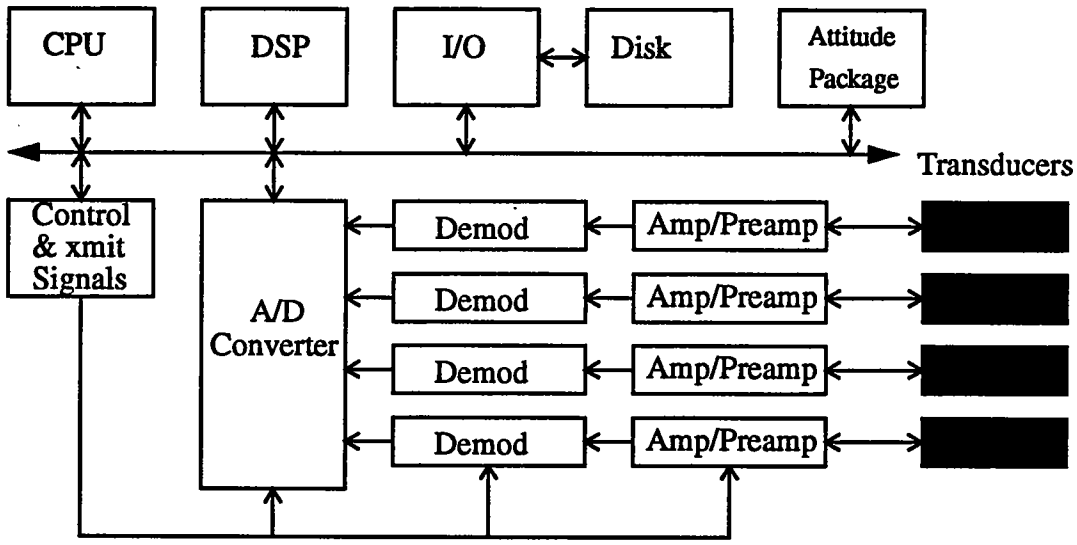

Figure 12 Electronics block diagram for the Doppler sonar. The block labeled Demod contains bandpass filtering, time varying gain and demodulation.

The amplifier card also contains the T/R network to separate the transmit and receive signals. It has one stage of programmable gain for setting the coarse gain range of the device depending on the backscatter intensity for a particular sea condition.

The backscatter signal is fed to four identical analog front-ends for demodulation, one for each transducer. The signals are amplified, quadrature demodulated and filtered. All the signals are then digitized by an A/D converter board. Carrier, demodulation, and sample clocks are all derived from a common source to ensure precise frequency and phase matching through all portions of the transmit and receive process. The sampled signals are then passed to the digital signal processor board to compute the sidescan intensity and to make the velocity estimates.

4.2.3 Data Storage

Long-term storage of data collected and processed by the system is accomplished using a standard SCSI hard disk or optical disk with at least 300 Mbytes capacity. For preliminary tests and short experiments the disk will be used to store all the raw data, for long-term experiments the sidescan and Doppler information will be stored as well as the wave directional spectra.

4.2.4 Sensors

In order to detect the motion and attitude of the package tilt sensors and a compass are included. Tilt sensors are used to check the vertical orientation of the package, and a compass is used to determine absolute direction. A rate gyro is necessary if mechanical

steering is done. A gyro is preferred in for use in a servo loop in order to 'lock-on' to a desired heading. A preliminary selection of sensors includes Lucas Accustar inclinometers, a KVH digital output fluxgate compass, and a Systron-Donner GyroChip angular rate sensor. All of these units are relatively low-cost, easy to use and compact.

5.0 Acknowledgments

The authors wish to acknowledge the contributions of D. Farmer, R. Pinkel, and J. Smith to the advancement of the surface-scanning sonar technique which have made possible the development of instruments like the one introduced here. In particular, the work of Smith (1989) helped to guide our thinking in this report. This work was supported by the Woods Hole Oceanographic Institution through a grant from the Webster Foundation.

6.0 References and Bibliography

[1] Brumley, B. H., R. G. Cabrera, K. L. Deines, and E. A. Terray, 1990, Performance of a broad-band acoustic doppler current profiler, Proceedings of the IEEE Fourth Working Conference on Current Measurement, IEEE, New York, 283-289.

[2] Crawford, G.B. and D.M. Farmer, 1987, On the spatial distribution of ocean bubbles. Journal of Geophysical Research, 92 (C8), 8231-8243.

[3] Farmer, D. M., R. C. Teichrob, C. J. Elder, and D. G. Sieberg, 1990. Novel acoustical instrumentation for the study of ocean surface processes. Oceans '90: Engineering in the Ocean Environment, Conference Proceedings, 11-17.

[4] Leibovich, S.A., 1983. The form and dynamics of Langmuir circulation. Annual Review of Fluid Mechanics, 15, 391-427.

[5] Miller, K. S. and M. M. Rochwarger, 1972. A covariance approach to spectral moment estimation. IEEE Transactions on Information Theory, IT-18 (5), 588-596.

[6] Pinkel, R., and J. A. Smith, 1987. Open ocean surface measurement using Doppler sonar. Journal of Geophysical Research, 92, 12,967-12,973.

[7] Pinkel, R., and J. A. Smith, 1992. Repeat-Sequence Coding for Improved Precision of Doppler sonar and Sodar. Journal of Atmospheric and Oceanic Technology, 9, 149-163.

[8] Plueddemann, A.J., D.M. Farmer, J. Smith, R.A. Weller, W.R. Crawford, R. Pinkel and S. Vagle, Oceanic observations of Langmuir circulation: From drifters to Doppler. in preparation for Journal of Geophysical Research.

[9] Pollard, R.T., 1977. Observations and theories of Langmuir circulations and their role in near surface mixing. A Voyage of Discovery, G. Deacon 70th Anniversary Volume, M. Angel, Ed., Pergammon Press, 235-251.

[10] Price, J.F., E.A. Terray, and R.A. Weller, 1987. Upper ocean dynamics. Reviews of Geophysics, 25, 193-203.

[11] Smith, J. A., 1989. Doppler sonar and surface waves: Range and resolution. Journal of Atmospheric and Oceanic Technology, 6, 680-696.

[12] Smith, J. A., 1992. Observed growth of Langmuir circulation. Journal of Geophysical Research, 97 (C4), 5651-5664.

[13] Smith, J.A., R. Pinkel, and R.A. Weller, 1987. Velocity structure in the mixed layer during MILDEX. Journal of Physical Oceanography, 17, 425-439.

[14] Thorpe, S.A., 1984. The effect of Langmuir circulation on the distribution of submerged bubbles caused by breaking wind waves. Journal of Fluid Mechanics, 142, 151-170.

[15] Thorpe, S.A., 1986. Measurements with an automatically recording inverted echo sounder: ARIES and the bubble clouds. Journal of Physical Oceanography, 16, 1462-1478.

[16] Thorpe, S. A., and A. J. Hall, 1983. The characteristics of breaking waves, bubble clouds, and near-surface currents observed using side-scan sonar. Continental Shelf Research, 1, 353--384.

[17] Thorpe, S. A., A. J. Hall, A. R. Packwood, and A. R. Stubbs, 1985. The use of a towed side-scan sonar to investigate processes near the sea surface. Continental Shelf Research, 4, 597-607.

[18] Weller, R. A., D. L. Rudnick, N. J. Pennington, R. P. Trask, and J. R. Valdez, 1990. Measuring upper ocean variability from an array of surface moorings in the Subtropical Convergence Zone. Journal of Atmospheric and Oceanic Technology, 7, 68--84.

[19] Weller, R. A., D. L. Rudnick, R. E. Payne, J. P. Dean, N. J. Pennington, and R. P. Trask, 1990. Measuring near-surface meteorology over the ocean from an array of surface moorings in the Subtropical Convergence Zone. Journal of Atmospheric and Oceanic Technology, 7, 85-103.

[20] Zedel, L., and D. Farmer, 1991. Organized structures in subsurface bubble clouds: Langmuir circulation in the open ocean. Journal of Geophysical, 96, 8889-8900.

7.0 Appendix: Matlab Functions

```
% arraysize.m   L. Freitag      WHOI, April 3, 1992
%
% computes and plots line array sizes for various beamwidths
% and frequencies.
% The equation used is:
%       dim = c/(f bw)
% where c is the speed of sound, f is frequency in Hz and bw
% is the beamwidth in degrees.
% A plot is made over the number of frequencies in input
% vector f with respect to the values in bw.
%
% function dim = arraysize(f,bw,c)

function dim = arraysize(f,bw,c)

  [m,n]=size(bw);
  C = c*ones(m,n)';

  for i=1:length(f)
    dim(:,i) = C./(f(i)*bw'*(pi/180));
  end;

  plot(bw,dim,'w-');

  grid;
  for i=1:length(f)
    s=sprintf('%2.0fkHz',f(i)/1000);
    text(min(bw),max(dim(:,i)),s);
 end;
 %text(0.7,0.88,'Frequency','sc');
 title('Array Size For Different Frequencies & Beamwidths');
 xlabel('Beam Width (deg)');
 ylabel('Array Size (m)');
```

```
% backscatter.m L. Freitag      WHOI, April 3, 1992
%
% computes and plots backscatter strength as a function of
% beamwidth and pulse length.
% The equation used is:
%       sstrength = 10 log(bw dR)       where dR = 0.5*c*T
% where c is the speed of sound,  bw is the
% beamwidth in degrees and T is the pulse length.
% A plot is made over the number of frequencies in input
% vector f with respect to the values in bw.
%
% function sstrength = backscatter(bw,T,c)

function sstrength = backscatter(bw,T,c)

  [m,n]=size(bw);
  C = c*ones(m,n)';
  bwrad= bw*pi/180;
  for i=1:length(T)
    sstrength(:,i) = 10*log10(bwrad'.*C*0.5*T(i));
  end;

  plot(bw,sstrength,'w-');

  grid;
  for i=1:length(T)
    s=sprintf('%2.0fmsec',T(i)*1000);
    text(min(bw),min(sstrength(:,i)),s);
 end;
 %text(0.7,0.88,'Frequency','sc');
 title('Backscatter Strength as a Function of Beamwidth
and Pulse Length');
 xlabel('Beam Width (deg)');
 ylabel('Backscatter Strength (dB)');
```

```
% cellsize.m    L. Freitag      WHOI, April 3, 1992
%
% computes and plots width of a cell for various beamwidths
% w.r.t range.
% The equation used is:
%       cell_size = 2*R*sin(alpha/2)
% where alpha is the beamwidth and R is the range
% example: cellsize([0.5 1 1.2 1.4 1.6 ],50:600);
% function cell_size = cellsize(alpha,R)

function cell_size = cellsize(alpha,R)

  for i=1:length(alpha)
    cell_size(:,i) = R'.*2*sin((alpha(i)/2)*(pi/180));
  end;

  plot(R,cell_size,'w-');

  grid;
  for i=1:length(alpha)
    s=sprintf('%2.1f',alpha(i));
    text(max(R),max(cell_size(:,i)),s);
 end;

 title('Cell Width For Different Array Beamwidths');
 ylabel('Cell Width (m)');
 xlabel('Range (m)');
```

```
% directivity.m L. Freitag      WHOI,   July, 1992
%
% computes and plots directivity index for different array
% dimensions
% Equation is from ITC literature and is an approximation
% function di = directivity(xbw,ybw)

function di = directivity(xbw,ybw)

  ybwrad = ybw*pi/180;
  xbwrad = xbw*pi/180;

  for i=1:length(ybw)
    di(:,i) = 10*log10(100*ones(xbw)./xbw)'
+ 10*log10(100/ybw(i)) + 5;
  end;

  plot(ybw,di,'w-');

  grid;
 for i=1:length(xbw)
   s=sprintf('%2.0f',xbw(i));
   text(max(ybw),min(di(i,:)),s);
 end;
 text(0.7,0.8,'X Beam Width (deg)','sc');
 title('Array Directivity Index for Different X-Y
Beamwidths');
 xlabel('Y Beam Width (deg)');
 ylabel('Directivity Index (dB)');
```

```
% pathloss.m    L. Freitag      WHOI, April 3, 1992
%
% computes and plots pathloss as a function of frequency
% and range. This accounts for spreading and attenuation
% The equation used is:
%       loss = 2*alpha*R + 30*logR
% where alpha is attenuation coef in db/m
% R is one-way range in meters.
% A plot is made over 100 to 300 kHz
%
% function loss = pathloss(R)

function loss = pathloss(R)
  % attenuation coefs from Smith, 1989 in dB/m
  f = [1e5 2e5 3e5];
  alpha = [0.03 0.06 0.08];

  for i=1:length(alpha)
    loss(:,i) = 2*alpha(i)*R' + 30*log10(R');
  end;

  plot(R,loss,'w-');

  grid;
  for i=1:length(f)
    s=sprintf('%2.0fkHz',f(i)/1000);
    text(max(R)-max(R)/10,max(loss(:,i)),s);
 end;
 %text(0.7,0.88,'Frequency','sc');
 title('Total Attenuation and Spreading Losses');
 xlabel('Range (m)');
 ylabel('Loss (dB)');
```

```
% powerlife.m   L. Freitag      WHOI, April 3, 1992
%
% computes and plots instrument life as a function of the
% number of measurements per day and the number of pings
% per measurement.
% This ignores quiescent electronics power over the course
% of the exp.
% The equation used is:
%       totalpower = TmIq2Vs + p2VsIpTp
% where time is converted accordingly to generate total
% watt-hours per measurement
% Inputs: Vs      one-sided amplifier supply voltage
%         Ip      peak current of amplifier (in amps)
%         Iq      quiescent current of power amp (in amps)
%         ntrans  number of transducers
%         pwidth  pulse width (in seconds)
%         ttime   pulse travel time (gvrns rep rate) (sec)
%                 (assumes ducers operate simultaneously)
%         npings  vector of number of pings per measurement
%         nmeas   vector of number of measurements per day
%         totbat  total battery power in W-H
%         dsppwr  power required by DSP & analog electronics
%

function totalpower = powerlife(Vs,Ip,Iq,ntrans,pwidth,
ttime,npings, nmeas, totbat, dsppwr)

  npings = npings';
  Tm = npings*ttime/3600   %total measurement time (hrs)

  for i=1:length(nmeas)
    totalpower(:,i) = nmeas(i) * (Tm*dsppwr+ Tm*2*Vs*Iq+
(pwidth*npings*ntrans/3600)*2*Vs*Ip);
  end;

  plot(nmeas,totalpower,'w-');

  grid;
  for i=1:length(npings)
    s=sprintf('%2.0f pings',npings(i));
    text(max(nmeas)-max(nmeas)/5,max(totalpower(i,:)),s);
  end;
  xc = 0.2;
  yc = 0.85;
  yinc = 0.03;
  text(0.15,0.88,'System Parameters:','sc');
  text(xc,yc,[num2str(ntrans) ' Transducers'],'sc');
  text(xc,yc-yinc,
['+/- ' num2str(Vs) ' Volts amp supply'],'sc');
  text(xc,yc-2*yinc,
```

```
[num2str(Ip) ' A peak amp current'],'sc');
  text(xc,yc-3*yinc,
[num2str(Iq*1000) ' mA amp quiescent'],'sc');
  text(xc,yc-4*yinc,
[num2str(pwidth*1000) ' msec pulse width '],'sc');
  text(xc,yc-5*yinc,
[num2str(ttime) ' sec RT travel time'],'sc');
  text(xc,yc-6*yinc,
[num2str(dsppwr) ' W Electronics Power'],'sc');
  text(xc,yc-7*yinc,
[num2str(totbat) ' W-H Battery Capacity'],'sc');

  title('Total (Active) System Power (wrt # Pings/Meas.)');
  xlabel('Measurements per Day');
  ylabel('Power Per Day (W-H)');
  pause;

  % Based on a given batter life compute inst. life
  [m,n]=size(totalpower);
  batmat = totbat*ones(m,n);
  explife = batmat./totalpower;
  semilogy(nmeas,explife,'w-');
  grid;
  for i=1:length(npings)
    s=sprintf('%2.0f pings',npings(i));
    text(min(nmeas),max(explife(i,:)),s);
  end;

  xc = 0.5;
  yc = 0.85;
  yinc = 0.03;
  text(0.45,0.88,'System Parameters:','sc');
  text(xc,yc,[num2str(ntrans) ' Transducers'],'sc');
  text(xc,yc-yinc,
['+/- ' num2str(Vs) ' Volts amp supply'],'sc');
  text(xc,yc-2*yinc,
[num2str(Ip) ' A peak amp current'],'sc');
  text(xc,yc-3*yinc,
[num2str(Iq*1000) ' mA amp quiescent'],'sc');
  text(xc,yc-4*yinc,
[num2str(pwidth*1000) ' msec pulse width '],'sc');
  text(xc,yc-5*yinc,
[num2str(ttime) ' sec RT travel time'],'sc');
  text(xc,yc-6*yinc,
[num2str(dsppwr) ' W Electronics Power'],'sc');
  text(xc,yc-7*yinc,
[num2str(totbat) ' W-H Battery Capacity'],'sc');

  title('Experiment Life for Fixed Battery Size
(w.r.t. # Pings/Meas.)');
```

```
xlabel('Measurements per Day');
ylabel('Experiment Life (days)');
hold on
%semilogy(nmeas,ones(nmeas)*365,'-w');
hold off
```

```
% velstd.m      L. Freitag      WHOI, April 3, 1992
%
% computes and plots standard deviation of velocity estimates
% for doppler systems. The equation used is:
%       sig = c/(4 pi f T)
% where c is the speed of sound, f is frequency in Hz and
% T is the pulse width in seconds.
% A plot is made over the number of frequencies in input
% vector f with respect to the values in T.
% Revised 5/7/93 to convert time to range resolution and plot
% xaxis in meters.
%
% function vstd = velstd(f,T,c)

function vstd = velstd(f,T,c)


  for i=1:length(f)
    for j=1:length(T)
     L = 0.5*(c*T(j));
     vstd(j,i)= (c*c)./(8*pi*f(i)*L);
    end;
  end;

%  axis([min(T*c)
  plot((T*c)/2,vstd,'w-');

  grid;
  for i=1:length(f)
    s=sprintf('%2.0fkHz',f(i)/1000);
    text(min((T*c)/2),max(vstd(:,i)),s);
 end;
 %text(0.7,0.88,'Frequency','sc');
 title('Standard Deviation of Velocity Est. (lower bound)
from Theriault');
 xlabel('Range Resolution (m)');
 ylabel('Velocity std. (m/sec)');
```

DOCUMENT LIBRARY

Distribution List for Technical Report Exchange – July 1, 1993

University of California, San Diego
SIO Library 0175C (TRC)
9500 Gilman Drive
La Jolla, CA 92093-0175

Hancock Library of Biology & Oceanography
Alan Hancock Laboratory
University of Southern California
University Park
Los Angeles, CA 90089-0371

Gifts & Exchanges
Library
Bedford Institute of Oceanography
P.O. Box 1006
Dartmouth, NS, B2Y 4A2, CANADA

Office of the International Ice Patrol
c/o Coast Guard R & D Center
Avery Point
Groton, CT 06340

NOAA/EDIS Miami Library Center
4301 Rickenbacker Causeway
Miami, FL 33149

Library
Skidaway Institute of Oceanography
P.O. Box 13687
Savannah, GA 31416

Institute of Geophysics
University of Hawaii
Library Room 252
2525 Correa Road
Honolulu, HI 96822

Marine Resources Information Center
Building E38-320
MIT
Cambridge, MA 02139

Library
Lamont-Doherty Geological Observatory
Columbia University
Palisades, NY 10964

Library
Serials Department
Oregon State University
Corvallis, OR 97331

Pell Marine Science Library
University of Rhode Island
Narragansett Bay Campus
Narragansett, RI 02882

Working Collection
Texas A&M University
Dept. of Oceanography
College Station, TX 77843

Fisheries-Oceanography Library
151 Oceanography Teaching Bldg.
University of Washington
Seattle, WA 98195

Library
R.S.M.A.S.
University of Miami
4600 Rickenbacker Causeway
Miami, FL 33149

Maury Oceanographic Library
Naval Oceanographic Office
Stennis Space Center
NSTL, MS 39522-5001

Library
Institute of Ocean Sciences
P.O. Box 6000
Sidney, B.C. V8L 4B2
CANADA

Library
Institute of Oceanographic Sciences
Deacon Laboratory
Wormley, Godalming
Surrey GU8 5UB
UNITED KINGDOM

The Librarian
CSIRO Marine Laboratories
G.P.O. Box 1538
Hobart, Tasmania
AUSTRALIA 7001

Library
Proudman Oceanographic Laboratory
Bidston Observatory
Birkenhead
Merseyside L43 7 RA
UNITED KINGDOM

IFREMER
Centre de Brest
Service Documentation - Publications
BP 70 29280 PLOUZANE
FRANCE

50272-101

REPORT DOCUMENTATION PAGE	1. REPORT NO. WHOI-93-23	2.	3. Recipient's Accession No.

4. Title and Subtitle
Design Study for a Moored Surface-Scanning Sonar

5. Report Date
June 1993

6.

7. Author(s) Lee E. Freitag, Albert J. Plueddemann, and Steve Merriam

8. Performing Organization Rept. No.
WHOI-93-23

9. Performing Organization Name and Address
Woods Hole Oceanographic Institution
Woods Hole, Massachusetts 02543

10. Project/Task/Work Unit No.

11. Contract(C) or Grant(G) No.
(C)
(G)

12. Sponsoring Organization Name and Address
Woods Hole Oceanographic Institution

13. Type of Report & Period Covered
Technical Report

14.

15. Supplementary Notes
This report should be cited as: Woods Hole Oceanog. Inst. Tech. Rept., WHOI-93-23.

16. Abstract (Limit: 200 words)

This report contains the results of a design study for a surface scanning sonar instrument capable of long-term deployment on ocean moorings. The instrument is intended to sample the bubble field just below the ocean's surface and compute the backscattered intensity and Doppler velocity in small unit volumes. The principal motivation for the development of such an instrument is to enhance the study of upper ocean processes by utilizing the ability of the sonar to detect surface waves and Langmuir circulation. Important design parameters for the instrument are investigated and a detailed design proposed. Key technical issues such as the trade-offs among spatial resolution, temporal resolution, velocity precision, total range, and power are discussed. The azimuthal motion of the instrument on a mooring is considered as a potential problem, and possible solutions are discussed. Matlab functions used for the investigations are included in an appendix.

17. Document Analysis **a. Descriptors**
Doppler sonar
surface scanning
moored instrumentation

b. Identifiers/Open-Ended Terms

c. COSATI Field/Group

18. Availability Statement
Approved for public release; distribution unlimited.

19. Security Class (This Report)
UNCLASSIFIED

20. Security Class (This Page)

21. No. of Pages
43

22. Price

(See ANSI-Z39.18) *See Instructions on Reverse*

OPTIONAL FORM 272 (4-77)
(Formerly NTIS-35)
Department of Commerce